



HAL
open science

Laser-guided lightning

Aurélien Houard, Pierre Walch, Thomas Produit, Victor Moreno, Benoit Mahieu, Antonio Sunjerga, Clemens Herkommer, Amirhossein Mostajabi, Ugo Andral, Yves-Bernard André, et al.

► **To cite this version:**

Aurélien Houard, Pierre Walch, Thomas Produit, Victor Moreno, Benoit Mahieu, et al.. Laser-guided lightning. Nature Photonics, 2023, 17, pp.231. 10.1038/s41566-022-01139-z . hal-03947576

HAL Id: hal-03947576

<https://hal.science/hal-03947576>

Submitted on 6 Feb 2023

HAL is a multi-disciplinary open access archive for the deposit and dissemination of scientific research documents, whether they are published or not. The documents may come from teaching and research institutions in France or abroad, or from public or private research centers.

L'archive ouverte pluridisciplinaire **HAL**, est destinée au dépôt et à la diffusion de documents scientifiques de niveau recherche, publiés ou non, émanant des établissements d'enseignement et de recherche français ou étrangers, des laboratoires publics ou privés.



Distributed under a Creative Commons Attribution 4.0 International License


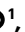






Laser-guided lightning

Received: 22 July 2022

Accepted: 29 November 2022

Published online: 16 January 2023

 Check for updates

Aurélien Houard ¹✉, Pierre Walch ¹, Thomas Produit ^{2,12}, Victor Moreno ², Benoit Mahieu¹, Antonio Sunjerga³, Clemens Herkommer⁴, Amirhossein Mostajabi³, Ugo Andral², Yves-Bernard André¹, Magali Lozano¹, Laurent Bizet¹, Malte C. Schroeder ², Guillaume Schimmel², Michel Moret², Mark Stanley⁵, W. A. Rison⁵, Oliver Maurice⁶, Bruno Esmler⁶, Knut Michel⁴, Walter Haas⁷, Thomas Metzger⁴, Marcos Rubinstein ⁸, Farhad Rachidi³, Vernon Cooray⁹, André Mysyrowicz^{1,10}, Jérôme Kasparian ^{2,11} & Jean-Pierre Wolf ²✉

Lightning discharges between charged clouds and the Earth's surface are responsible for considerable damages and casualties. It is therefore important to develop better protection methods in addition to the traditional Franklin rod. Here we present the first demonstration that laser-induced filaments—formed in the sky by short and intense laser pulses—can guide lightning discharges over considerable distances. We believe that this experimental breakthrough will lead to progress in lightning protection and lightning physics. An experimental campaign was conducted on the Säntis mountain in north-eastern Switzerland during the summer of 2021 with a high-repetition-rate terawatt laser. The guiding of an upward negative lightning leader over a distance of 50 m was recorded by two separate high-speed cameras. The guiding of negative lightning leaders by laser filaments was corroborated in three other instances by very-high-frequency interferometric measurements, and the number of X-ray bursts detected during guided lightning events greatly increased. Although this research field has been very active for more than 20 years, this is the first field-result that experimentally demonstrates lightning guided by lasers. This work paves the way for new atmospheric applications of ultrashort lasers and represents an important step forward in the development of a laser based lightning protection for airports, launchpads or large infrastructures.

Lightning has fascinated and terrified humankind since time immemorial. Based on satellite data, the total lightning flash rate worldwide—including cloud-to-ground and cloud lightning—is estimated to be between 40 and 120 flashes per second¹, causing considerable damage and casualties. The documented number of lightning fatalities is well above 4,000 (ref. 2) and lightning damages amount to billions of dollars every year³. The most widely used external protection against direct lightning strikes is still the lightning rod, also known as Franklin

rod or lightning conductor. The lightning rod, whose invention in the 18th century is attributed to Benjamin Franklin, consists of a pointed conducting mast connected to the ground. It protects buildings and their immediate surroundings by providing a preferential strike point for the lightning and guiding its electric current safely to the ground.

A method to initiate lightning discharges with a small rocket trailing a long, grounded conducting wire was demonstrated by Newman et al. in 1965 (ref. 4). In contrast to the classical lightning rod, which

A full list of affiliations appears at the end of the paper. ✉e-mail: aurelien.houard@polytechnique.edu; jean-pierre.wolf@unige.ch



Fig. 1 | Image of the 124-m-high telecommunication tower of Säntis (Switzerland). Also shown is the path of the laser recorded with its second harmonic at 515 nm.

is intended to be struck by lightning that approaches the protected structure, the rocket-and-wire technique is intended to trigger lightning artificially. Rapidly inserting a wire into the strong electric fields near the ground below a thundercloud results in a field at the tip of the wire sufficiently enhanced to produce electrical breakdown. If the small rocket is fired at the right moment when conditions for lightning are met, this method can initiate lightning with a success rate of up to 90% (ref. 5). However, it requires expendable rockets and wires, the falling debris of which presents a danger.

The idea of using a laser to trigger lightning was first suggested by Ball⁶. A first attempt to trigger and guide natural lightning with lasers was made by Uchida et al. in 1999 using a combination of three lasers with kilojoule energy to form a 2-m-long plasma spark^{7–9}. In this Article we present results of a campaign relying on the use of laser filamentation. The principle of the filament lightning rod is the following: intense and short laser pulses are sent toward the clouds. They undergo a filamentation process during their propagation^{10–12}. The laser pulse first shrinks in size because of the laser-induced change of the refractive index of the air, which acts like a self-generated series of increasingly converging lenses. The laser pulse eventually becomes sufficiently intense to ionize air molecules in a high-field process. Further propagation of the laser pulse is ruled by a dynamic competition between beam self-focusing and the defocusing effect due to the presence of free electrons. This competition maintains narrow channels of ionizing

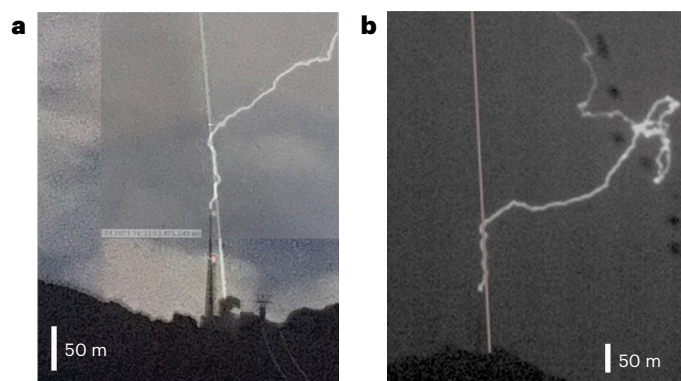


Fig. 2 | Snapshots of the lightning event of 24 July 2021 (L2) recorded in the presence of the laser. **a, b**, Snapshot recorded by the two high-speed cameras located at Schwaegalp (**a**) and Kronberg (**b**). The trajectory of the laser path taken subsequently in clear sky through second harmonic generation is also overlaid.

laser pulses over long distances. Along these filamentary regions, air molecules are rapidly heated by the absorbed laser energy and expelled radially at supersonic speed, leaving behind long-lived channels of air with reduced density^{13–17}. These low-density channels of millisecond duration have higher electronic conductivity and consequently offer a privileged path for electric discharges. Metres-long electric discharges triggered and guided by filaments have been demonstrated in the laboratory^{18–23} and they have been shown to compete successfully with traditional lightning rods²⁴. The ionized length of filamentation can reach a hundred metres when the initial pulse power of picosecond duration is in the terawatt (10^{12} W) range^{25,26}. The filamentation process can be controlled so that it starts up to a kilometre away from the laser source^{26,27}. It is therefore conceivable that filamentary channels can serve to guide and possibly even to trigger lightning discharges under appropriate weather conditions.

In our experimental campaign performed during the summer of 2021, a Yb:YAG laser emitting pulses of picosecond duration and 500 mJ energy at a wavelength of 1,030 nm and at 1 kHz repetition rate²⁸ was installed in the vicinity of a 124-m-tall telecommunications tower located on top of the Säntis mountain in north-eastern Switzerland (see refs. 29, 30, Methods, and Extended Data Figs. 1 and 2 for a description of the experimental set-up). This tower, which is struck by lightning about 100 times a year, is equipped with multiple sensors to record the lightning current, electromagnetic fields at various distances, X-rays and radiation sources from the lightning discharges (see refs. 31–34 for a detailed description of the lightning instrumentation). The laser pulses were directed upward, with a propagation path passing in the vicinity of the tip of the tower, which is equipped with a Franklin rod (see Fig. 1). Relying on the results of a preliminary horizontal propagation campaign in laboratory, the laser conditions were adjusted so that initiation of filamentary behaviour started close to, but above the tip of the tower, and had a length of at least 30 m.

Between 21 July and 30 September 2021, the laser was operated during a total of 6.3 h of thunderstorm activity occurring within 3 km of the tower. The tower was hit by at least 16 lightning flashes, four of which—denoted L1, L2, L3 and L4 (see Extended Data Table 1 for a list of the lightning events)—occurred during laser activity. All of the recorded lightning strikes were upward, in accordance with 97% of the strikes observed at the Säntis Tower since 2010 (ref. 35). However, although observations at the Säntis Tower over nine years in the absence of a laser show 84% negative, 11% positive and 5% bipolar flashes³⁶, the four recorded laser events were all positive flashes, connecting the top of the tower to a positive charge centre in the cloud. According to the atmospheric electricity sign convention, a positive (negative) lightning flash is produced by a positively (negatively) charged cloud and generates

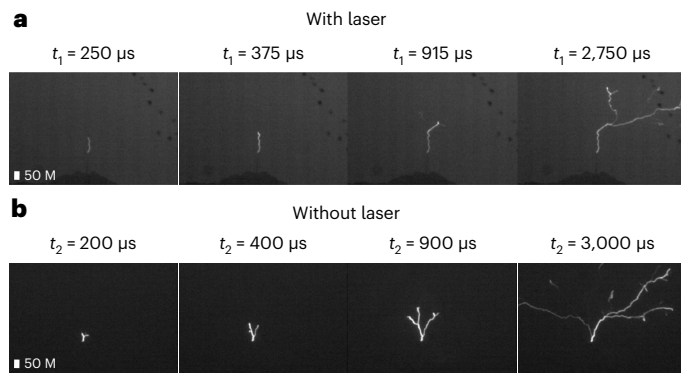


Fig. 3 | High-speed camera images of upward leaders. **a**, Images of the lightning path in the presence of the laser recorded on 24 July 2021 (L2) at 250, 375, 915 and 2,750 μs after initiation of the discharge. **b**, Images of the lightning path recorded on 2 July 2019 in the absence of a laser 200, 400, 900 and 3,000 μs after initiation of the discharge.

a positive (negative) background electric field around the tower; it can then induce upward negative (positive) leaders. Only one of these four laser events (L2) occurred during a relatively clear sky on 24 July 2021 at 16:24 UTC, which allowed us to record the path of the lightning discharge from two directions with two high-speed cameras located 1.4 and 5 km from the tower, respectively. Snapshots of this event are displayed in Fig. 2. They show that the lightning strike initially follows the laser path over most of the initial 50 m distance (see also Extended Data Fig. 3). Notice that the discharge is not completely straight along this initial segment, as it would be when triggering lightning with a rocket trailing a wire. This difference is, however, well known from laser triggered and guided discharges performed at High Voltage facilities³⁷. The reason is that the current displacement is much more complex in a distribution of moving charges than along a wire. For instance, the moving charges create space charges that locally screen the electric field. Figure 3 shows time-resolved sequences of ascending negative leaders for two upward flashes, one (L2) that occurred with the laser in operation and the other without the laser on 2 July 2019 at 00:22 UTC. Note the absence of branching during the laser guiding stage (lowest vertical section) of L2.

A lightning storm is the source of emission of electromagnetic waves spanning a broad frequency range from radio waves to gamma-rays. Very-high-frequency (VHF) activity (of 1–10 m wavelength) is particularly useful for the study of discharges during their formation stage. A VHF interferometer system developed by New Mexico Tech was installed during the 2021 summer measurement campaign in the vicinity of the Säntis Tower³⁸. This system consists of inverted V-shape antennas recording the phase differences between incoming VHF radiation sources due to their different locations. By using a cross-correlation algorithm³⁹, the location of the source can be obtained in a two-dimensional space (azimuth, elevation). The system was capable of tracking the lightning leader propagation with a spatial resolution of several metres and a time resolution on the order of microseconds. Figure 4 compares the VHF sources located by the interferometer for two flashes: one (L1) with the laser active and the other without the laser (N07). In the former scenario, an accumulation of radiation sources located along the laser path is observed over a distance of approximately 60 m (other events are presented in Extended Data Fig. 4). As presented in Extended Data Table 2 and Fig. 5, the standard deviation of the distance from the sources to the laser is reduced by 45% over the same 60 m when the laser is on.

The lightning current, electric fields and X-rays were observed for the L1, L3 and L4 events. Results for L1 and L3 are presented in Fig. 5 and compared to an event with the same positive polarity measured in the absence of laser. The X-ray detector field of view was pointing toward

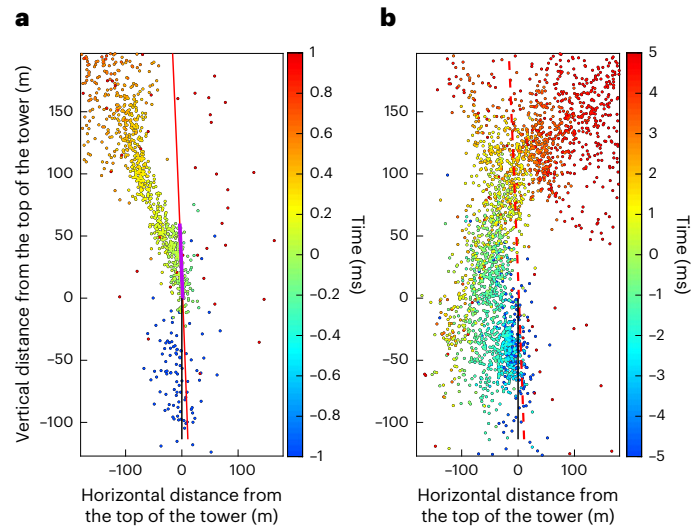


Fig. 4 | Measurements with VHF interferometer. **a, b**, Two-dimensional maps of the VHF sources emitted during the lightning event L1 with the laser on (**a**) and event N6 without the laser (**b**). The telecommunication tower is in black whereas the laser path is in red (continuous red line when the laser is present, and dashed red line when the laser is off). Each point corresponds to a VHF emission. The colour scale bars displayed on the right correspond to the timescale. The violet section shows the region in which laser filamentation is expected.

the laser trajectory. The three events presented here were compared with two other positive upward events during 2021 before the laser installation. They exhibited similar current and electric field waveforms in terms of amplitudes and step intervals. On the other hand, the number of X-ray bursts in the presence of the laser beam (4.3 per event) was much higher than in its absence (one per event). Note that most of the X-ray bursts observed with the laser on are detected during the time corresponding to the laser-guided leader propagation (first 500 μs). Unpublished experiments performed at the Laboratoire d'Optique Appliquée, show that metre-long guided discharges emit an X-ray burst in the forward direction. This suggests that these X-ray bursts were emitted during straight sections of the discharge (see Fig. 2).

Discussion of the results

Before the 2021 campaign described in this paper, a few attempts at guiding and/or initiating lightning using short laser pulse filaments with terawatt peak power were made in New Mexico in 2004 (ref. 40), and in Singapore in 2011. These earlier campaigns failed to produce evidence of laser guiding or initiation of lightning discharges. This raises the following two questions: (1) why was the Säntis campaign more successful than the two previous attempts? And (2) why were only upward negative leaders (associated with upward positive flashes) guided by the laser during this campaign?

We conjecture that an important factor contributing to the success of the Säntis campaign is the repetition rate of the laser, which was higher by two orders of magnitude when compared with previous attempts. Before a lightning flash at Säntis, the electric field is typically varying very slowly (tens to hundreds of milliseconds). This is because most of the flashes are self-initiated⁴¹. Using a kilohertz repetition rate therefore allows interception of all of the lightning precursors developing above the tower. Furthermore, during filamentation, a small fraction of the free electrons created by high-field ionization is captured by neutral oxygen molecules. At high laser repetition rates, these long-lived charged oxygen molecules accumulate, keeping a memory of the laser path⁴². Electrons captured by neutral oxygen molecules have a trapping potential of 0.15 eV (ref. 43) instead of 13.62 and 15.58 eV for electrons bound to oxygen and nitrogen molecules, respectively, and they can therefore easily be set free by heat or inelastic collisions with

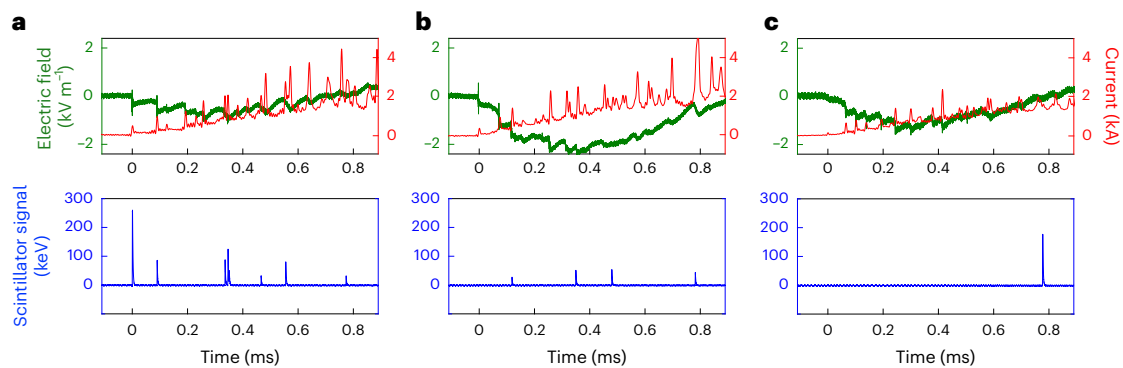


Fig. 5 | Electric signals measured for the three positive upward flashes. **a–c**, Electric signals measured for the three positive upward flashes L1 (**a**), L3 (**b**) and N6 (**c**). Top: the electric field scale is given on the left y-axis and the current on the right y-axis. Bottom: X-ray signals detected by the scintillator,

where each peak corresponds to the integrated X-rays energy collected during the 50 ns sampling. Events L1 and L3 correspond to events with a laser, whereas N6 corresponds to an event without a laser.

energetic electrons accelerated by the ambient electric field. Laboratory experiments have provided evidence of the presence of such free electrons in filaments at kilohertz laser repetition rate⁴⁴. Filaments with an accumulation of positively and negatively charged molecules as well as free electrons form a polarizable medium. Charge migration inside the filament strings, induced by the atmospheric electric field, can produce a reinforcement of the electric field, promoting the formation of discharge segments⁴⁵. More campaigns and theoretical work are necessary to confirm this conjecture.

To explain why only negatively charged ascending leaders (positive lightning flashes) were observed in the presence of the laser beam, it is instructive to consider the electric field conditions required to generate a discharge bridging the gap between the lower tip of the filamentary path and the metallic rod at the top of the tower (see Methods for details on the model). Consider first the case in which the background electric field is generated by positive charges in the cloud. In this scenario the gap could be bridged either by negative streamers emanating from the tower tip or by positive streamers generated by the lower tip of the laser filament. Our calculations, based on the conditions necessary for the initiation and propagation of streamer discharges (see Supplementary Information), show that bridging the gap by positive streamers emanating from the bottom tip of the filament takes place at a lower background electric field (denoted $E_{\text{pos-filament}}$) in comparison with the electric field needed to bridge the gap by negative streamers. Note that this scenario will give rise to a positive lightning flash.

Now let us consider the case in which the background electric field is generated by negative charges in the cloud. Again, two scenarios are possible: the gap could be bridged either by positive streamers initiated from the tower tip or by negative streamers initiated from the lower tip of the filament. As before, positive streamers—emanating now from the tower—bridge the gap at a lower electric field denoted $E_{\text{pos-tower}}$, giving rise to negative lightning flashes. Furthermore, our calculations show that $E_{\text{pos-filament}} < E_{\text{pos-tower}}$. This means that positive lightning flashes are more likely to be initiated in the presence of the laser filaments than negative flashes. Note that the same tendency has been observed in the laboratory, where the triggering of metre scale discharges by laser filaments was studied with positive and negative polarities²⁴.

In conclusion, the results of the Sântis experimental campaign in the summer of 2021 provide circumstantial evidence that filaments formed by short and intense laser pulses can guide lightning discharges over considerable distances. These preliminary results should be confirmed by additional campaigns with new configurations. The use of a Franklin rod with a minimum distance from the laser path could increase the probability to guide lightning flashes of both polarities.

The use of visible laser wavelengths (obtained by second harmonic generation) could also increase the guiding efficiency of the filament. Also note that, based on the results presented in this paper, displacing the onset of filamentation toward charge centres in the cloud might result in an increase in the guiding capability of the laser or even the initiation of lightning discharges. This is the subject of future experimental work.

Online content

Any methods, additional references, Nature Portfolio reporting summaries, source data, extended data, supplementary information, acknowledgements, peer review information; details of author contributions and competing interests; and statements of data and code availability are available at <https://doi.org/10.1038/s41566-022-01139-z>.

References

1. Turman, B. N. & Edgar, B. C. Global lightning distributions at dawn and dusk. *J. Geophys. Res.* **87**, 1191–1206 (1982).
2. Holle, R. L. The number of documented global lightning fatalities. In *24th International Lightning Detection Conference (ILDC)* (2016).
3. Holle, R. L. Some aspects of global lightning impacts. In *2014 International Conference on Lightning Protection (ICLP)* 1390–1395 (IEEE, 2014).
4. Newman, N. M. in *Problems of Atmospheric and Space Electricity* 482–490 (Elsevier, 1965).
5. Gary, C. *La Foudre* 2nd edn (Masson, 1999).
6. Ball, L. M. The laser lightning rod system: thunderstorm domestication. *Appl. Opt.* **13**, 2292–2295 (1974).
7. Wang, D. et al. A possible way to trigger lightning using a laser. *J. Atmos. Terr. Phys.* **57**, 459–466 (1995).
8. Uchida, S. et al. Laser-triggered lightning in field experiments. *J. Opt. Technol.* **66**, 199–202 (1999).
9. Rakov, V. A. & Uman, M. A. *Lightning: Physics and Effects* (Cambridge Univ. Press, 2003).
10. Chin, S. L. et al. The propagation of powerful femtosecond laser pulses in optical media: physics, applications, and new challenges. *Can. J. Phys.* **83**, 863 (2005).
11. Couairon, A. & Mysyrowicz, A. Femtosecond filamentation in transparent media. *Phys. Rep.* **441**, 47–189 (2007).
12. Bergé, L. S., Skupin, R., Nuter, J., Kasparian & Wolf, J.-P. Ultrashort filaments of light in weakly ionized, optically transparent media. *Rep. Prog. Phys.* **70**, 1633 (2007).
13. Vidal, F. et al. Modeling the triggering of streamers in air by ultrashort laser pulses. *IEEE Trans. Plasma Science* **28**, 418–433 (2000).

14. Tzortzakis, S. et al. Femtosecond laser-guided electric discharge in air. *Phys. Rev. E* **64**, 57401 (2001).
15. Cheng, Y.-H., Wahlstrand, J. K., Jhaji, N. & Milchberg, H. M. The effect of long timescale gas dynamics on femtosecond filamentation. *Opt. Express* **21**, 4740–4751 (2013).
16. Lahav, O. et al. Long-lived waveguides and sound-wave generation by laser filamentation. *Phys. Rev. A* **90**, 021801(R) (2014).
17. Point, G., Milián, C., Couairon, A., Mysyrowicz, A. & Houard, A. Generation of long-lived underdense channels using femtosecond filamentation in air. *J. Phys. B* **48**, 094009 (2015).
18. Diels, J.-C., Bernstein, R., Stahlkopf, K. E. & Zhao, X. M. Lightning control with lasers. *Sci. Am.* **277**, 50–55 (1997).
19. Comtois, D. et al. Triggering and guiding leader discharges using a plasma channel created by an ultrashort laser pulse. *Appl. Phys. Lett.* **76**, 819 (2000).
20. Rodriguez, M. et al. Triggering and guiding megavolt discharges by use of laser-induced ionized filaments. *Opt. Lett.* **27**, 772–774 (2002).
21. Kasparian, J. et al. White-light filaments for atmospheric analysis. *Science* **301**, 61–64 (2003).
22. Fuji, T. et al. Leader effects on femtosecond-laser-triggered discharges. *Phys. Plasma* **15**, 013107 (2008).
23. Wolf, J.-P. Short-pulse lasers for weather control. *Rep. Prog. Phys.* **81**, 026001 (2018).
24. Forestier, B. et al. Triggering, guiding and deviation of long air spark discharges with femtosecond laser filament. *AIP Adv.* **2**, 012151 (2012).
25. Méchain, G. et al. Range of plasma filaments created in air by a multi-terawatt femtosecond laser. *Opt. Commun.* **247**, 171–180 (2005).
26. Durand, M. et al. Kilometer range filamentation. *Opt. Express* **21**, 26836 (2013).
27. Rodriguez, M. et al. Kilometer-range nonlinear propagation of femtosecond laser pulses. *Phys. Rev. E* **69**, 36607 (2004).
28. Herkommer, C. et al. Ultrafast thin-disk multipass amplifier with 720 mJ operating at kilohertz repetition rate for applications in atmospheric research. *Opt. Express* **28**, 30164 (2020).
29. Produit, T. et al. The laser lightning rod project. *Eur. Phys. J. Appl. Phys.* **93**, 10504 (2021).
30. Produit, T. De la réalisation d'un paratonnerre laser. PhD thesis. Univ. Genève (2021).
31. Romero, C. et al. Measurement of lightning currents using a combination of Rogowski coils and B-dot sensors. In *2010 30th International Conference on Lightning Protection (ICLP) 1–5* (IEEE, 2010); <https://doi.org/10.1109/ICLP.2010.7845959>
32. Romero, C. et al. A system for the measurements of lightning currents at the Sântis Tower. *Electr. Power Syst. Res. J.* **82**, 34–43 (2012).
33. Azadifar, M. et al. An update on the instrumentation of the Sântis Tower in Switzerland for lightning current measurements and obtained results. In *International Colloquium on Lightning and Power Systems* (CIGRE, 2014).
34. Sunjerga, A. et al. Sântis Lightning Research Facility instrumentation. In *Joint 35th International Conference on Lightning Protection (ICLP) and 16th International Symposium on Lightning Protection (SIPDA) 20–26* (SIPDA, 2021).
35. Romero, C., Rachidi, F., Paolone, M. & Rubinstein, M. Statistical distributions of lightning current parameters based on the data collected at the Sântis Tower in 2010 and 2011. *IEEE Trans. Power Deliv.* **28**, 1804 (2013).
36. Rachidi, F. & Rubinstein, M. Sântis lightning research facility: a summary of the first ten years and future outlook. *Elektrotech. Inf.* **139**, 379–394 (2022).
37. Ackermann, R. et al. Influence of negative leader propagation on the triggering and guiding of high voltage discharges by laser filaments. *Appl. Phys. B* **82**, 561–566 (2006).
38. Stanley, M. A. et al. Initial results from a 2nd generation Broadband VHF Interferometer Imaging system. In *AGU Fall Meeting 1–17* (AGU, 2020).
39. Stock, M. G. et al. Continuous broadband digital interferometry of lightning using a generalized cross-correlation algorithm. *JGR Atmos.* **119**, 3134 (2014).
40. Kasparian, J. et al. Electric events synchronized with laser filaments in thunderclouds. *Opt. Express* **16**, 5757 (2008).
41. Smorgonskiy, A. et al. An analysis of the initiation of upward flashes from tall towers with particular reference to Gaisberg and Sântis Towers. *J. Atmos. Sol.-Terr. Phys.* **136**, 46–51 (2015).
42. Walch, P. et al. Cumulative air density depletion during high repetition rate filamentation of femtosecond laser pulses: Application to electric discharge triggering. *Appl. Phys. Lett.* **119**, 264101 (2021).
43. Burch, D. S., Smith, S. J. & Branscomb, L. M. Photodetachment of O₂⁻. *Phys. Rev.* **112**, 171 (1958).
44. Schubert, E., Mongin, D., Kasparian, J. & Wolf, J.-P. Remote electrical arc suppression by laser filamentation. *Opt. Express* **23**, 28640–28648 (2015).
45. Zhao, X. M., Diels, J. C., Wang, C. Y. & Elizondo, J. Femtosecond ultraviolet laser pulse induced lightning discharges in gases. *IEEE J. Quant. Elec.* **31**, 599 (1995).

Publisher's note Springer Nature remains neutral with regard to jurisdictional claims in published maps and institutional affiliations.

Open Access This article is licensed under a Creative Commons Attribution 4.0 International License, which permits use, sharing, adaptation, distribution and reproduction in any medium or format, as long as you give appropriate credit to the original author(s) and the source, provide a link to the Creative Commons license, and indicate if changes were made. The images or other third party material in this article are included in the article's Creative Commons license, unless indicated otherwise in a credit line to the material. If material is not included in the article's Creative Commons license and your intended use is not permitted by statutory regulation or exceeds the permitted use, you will need to obtain permission directly from the copyright holder. To view a copy of this license, visit <http://creativecommons.org/licenses/by/4.0/>.

© The Author(s) 2023

¹Laboratoire d'Optique Appliquée – ENSTA Paris, Ecole Polytechnique, CNRS, IP Paris, Palaiseau, France. ²Groupe de Physique Appliquée, Université de Genève, Geneva, Switzerland. ³EMC Laboratory, Electrical Engineering Institute, Ecole Polytechnique Fédérale de Lausanne (EPFL), Lausanne, Switzerland. ⁴TRUMPF Scientific Lasers GmbH + Co. KG, Unterföhring, Germany. ⁵Langmuir Laboratory for Atmospheric Research, New Mexico Institute of Mining and Technology, Socorro, NM, USA. ⁶ArianeGroup, Les Mureaux, France. ⁷Swisscom Broadcast AG, Bern, Switzerland. ⁸School of Management and Engineering Vaud, University of Applied Sciences and Arts Western Switzerland, Yverdon-les-Bains, Switzerland. ⁹Department of Electrical Engineering, Uppsala University, Uppsala, Sweden. ¹⁰André Mysyrowicz Consultants, Versailles, France. ¹¹Institute for Environmental Sciences, Université de Genève, Geneva, Switzerland. ¹²Present address: Institute of Materials Research and Engineering, Agency for Science Technology and Research (A*STAR), Singapore, Singapore. ✉e-mail: aurelien.houard@polytechnique.edu; jean-pierre.wolf@unige.ch

Methods

Laser system

The laser system operating during the campaign—fully described in ref. 28—is a Yb:YAG Chirped pulse amplification laser system developed by TRUMPF Scientific Lasers. It is capable of delivering laser pulses at 1,030 nm with 720 mJ of energy per pulse, a pulse duration of 920 fs at a repetition rate of 1 kHz. Due to the configuration of our set-up, which features a long propagation before the sending telescope, the output energy was reduced to 500 mJ and the pulse was chirped to a pulse duration of 7 ps to prevent damage to the optics. In Extended Data Fig. 1b, an lithium triborate crystal⁴⁶ was used to produce a beam at the second harmonic at 515 nm wavelength.

Experimental set-up

The campaign was performed at the top of the Säntis mountain (2,502 m altitude) in north-eastern Switzerland, on the summit of which stands a 124-m-tall telecommunication tower. A general view of the experimental set-up is presented in Extended Data Fig. 1. The laser system was located in the radome building, sheltered in an air-tight, air-conditioned and thermally isolated tent. After exiting the tent, the laser output was directed downwards by a conduit through the radome wall to the terrace, where a 4' folding mirror directed the beam into a beam-expanding sending telescope featuring a 7.14 magnification ratio. The entire laser path toward the telescope—presented in Extended Data Fig. 1a—was protected by an isolated aluminium housing to prevent any beam leakage and to reduce the perturbation from the environment.

The telescope was composed of an additional folding mirror, a secondary 100 mm spherical mirror and a 430-mm diameter off-axis aspheric (elliptic) primary mirror²⁹. The beam output, which had a diameter of 250 mm, was sent toward the tower tip with a vertical angle of 7°. Translation stages on the secondary mirror allowed us to focus the beam near the tower tip in order to set the onset of the filamentation process in the desired area in which upward lightning is initiated. The focal length of the telescope was set to 150 m to produce a dense filamentation area of 30–50 m above the tower tip.

Note that during the entire laser operation time, the airspace was closed by the air-traffic authority. Furthermore, air traffic was monitored by an automatic dependent surveillance–broadcast transceiver automatically switching off the laser in case of aircraft incursion into the temporary closed airspace zone.

High-speed camera measurements

On 24 July, 2021 the L2 event was observed with the two high-speed cameras: one operating at 24,000 fps, installed on the Kronberg mountain; and the second operating at 10,000 fps, installed at Säntis Das Hotel (Schwaegalp). Note that high-speed camera records of upward positive flashes are very rare and there are only a few reported in the literature^{47,48}.

Figure 2 displays two representative frames taken from the two fast cameras. Several comparative procedures were performed to precisely calibrate the position of the laser: images from the fast cameras in daylight to identify the position of the tower and the surrounding topography; high resolution pictures at night with a D810 Nikon next to the fast cameras when the laser was operating; and reconstruction of the laser direction and position using precise GPS data. In the two pictures in Fig. 2, which depict an upward positive flash, an initial segment of about 70 m from Schwaegalp and 120 m from Kronberg is observed, following the path of the laser beam.

For events without a laser, individual images from one of the cameras were available, allowing us to plot the histograms of the distances to the laser beam as projected in the plane perpendicular to the camera line of sight (Extended Data Fig. 3). The difference in behaviour between the event with (L2) and without a laser (N08, N08) is apparent.

Leader velocity

The velocity estimated from the interferometer data (between 1×10^5 and 6×10^5 m s⁻¹) is consistent with estimates deduced from the 24,000 fps image sequence of the fast camera located in Kronberg, which yields a velocity decaying from 4×10^5 m s⁻¹ when leaving the tower tip to 9×10^4 m s⁻¹ at the first branching 120 m above it, with an average velocity of 2×10^5 m s⁻¹ over this interval. Unfortunately, no fast camera image was available under comparable conditions (upward positive flash) without the laser during the campaign. This value is, however, comparable with the typical reported values for upward negative leaders (corresponding to positive flashes): 2×10^5 m s⁻¹ for rocket-triggered lightning⁴⁹ and 1×10^5 m s⁻¹ for virgin air⁵⁰. Note that from the fast camera images, the propagation velocity of the branches of the laser-free event of 2 July 2019 00:22:46 is estimated to be 2×10^5 m s⁻¹, without any discernible acceleration or deceleration trend over the first 900 m.

Modelling and simulation of the effect of the filamentation on the lightning flashes initiation

To understand the conditions necessary for the initiation of a lightning flash in the presence of the laser filament, we will describe below the physical processes that are involved^{51,52}. We will start by presenting the standard nomenclature used in the lightning literature. When the electric field in air exceeds the breakdown electric field, the free electrons in the air start ionizing other atoms and molecules, giving rise to what is commonly known as an electron avalanche. As the avalanche continues to grow, a stage will be reached where the accumulated space charge becomes so large that it starts creating electric fields comparable with, or higher than, the background electric field. At this stage the electron avalanche becomes a self-propagating electrical discharge known as a streamer. Streamers can propagate in background electric fields lower than the breakdown values. The currents in these streamer discharges are in the micro- to milliamperes range. Moreover, streamers are cold discharges. That is, the temperature of the gas in the discharge remains close to the ambient temperature. During the initiation of a discharge, many streamers may originate from a common root or stem. As the current from all of the streamers passes through this stem, the temperature of the stem increases. As the stem heats up, thermal ionization sets in, increasing the electron density in the stem. When this electron density reaches a critical density, a rapid transfer of energy from the electrons to the neutral atoms takes place, raising the conductivity and the temperature of the gas to several thousands of degrees. This conducting channel section is called a leader. Being conducting, this channel gets polarized in the background electric field, thus enhancing the electric field at its tip. From this tip, an electron avalanche starts again, leading to the creation of a new section of the leader channel. In this way, with the aid of avalanches and streamers, the leader propagates. When a downward lightning leader reaches the ground or attaches to an upward connecting leader, a ground potential wave called return stroke propagates along the leader channel neutralizing its charge. This return stroke constitutes the visible and audible phase of the lightning strike. The processes that were just described are the main elements that are being used to describe the mechanism of lightning flashes.

Now let us consider the problem at hand. We shall estimate whether there will be electrical breakdown between the lower end of the laser filament and the tower tip, a step which is necessary for the initiation of a lightning discharge by the laser filament. This evaluation contains many steps and it is not possible to describe all of them in detail here. The interested reader may find a full discussion in references^{51–53}. However, we will describe the essential elements here while at the same time providing the references for the interested reader to go deeper into the analysis. First, for a given background electric field, the electric field in the gap between the tower tip and the lower tip of the filament is calculated using the charge simulation method. This is a standard technique to calculate the electric field in a region

where the potential boundaries are given⁵⁴. Second, the growth of electron avalanches in the high electric field region where the electric field exceeds the breakdown electric field is studied⁵⁵. The growth of avalanches is investigated using the Townsend ionization coefficient corresponding to the ambient pressure and temperature. Third, if the number of positive ions at the electron avalanche head exceeds the critical value of 10^8 , within a roughly spherical region of 50 μm radius, the avalanche is assumed to be converted to a streamer discharge⁵⁶. Fourth, once a streamer is initiated, its propagation distance into the gap is estimated using the value of the critical electric field necessary for streamer propagation. For the propagation of positive streamers at mean sea-level pressure, a background electric field of about 500 kV m^{-1} is required and, for negative streamers, the required field is higher: 1 MV m^{-1} to 2 MV m^{-1} (refs. 57, 58). Both of these values have to be scaled by a factor of 0.75 to take into account the 0.75 atm pressure at the 2,500 m altitude of the Säntis Tower. Once the extension of the streamers in the gap is estimated, the charge associated with the streamer burst is estimated following the procedure used by Becerra and Cooray⁵⁹. If the charge in the streamer burst is larger than 1 μC , the streamer burst will give rise to a leader discharge⁵⁶. Leaders can propagate in fields larger than about 150–200 kV m^{-1} which is much lower than the threshold necessary for streamer propagation^{57,58,60}. Based on this procedure, the analysis to be presented below is carried out.

Consider the location of a laser filament above the tip of the tower. The geometry relevant to the calculation is shown in Extended Data Fig. 6. In the case of a laser filament fully polarized by the background electric field, the conditions necessary for the initiation of a lightning flash are the following. First, a streamer burst has to be initiated from the lower tip (the tip closest to the tower) of the laser filament. This streamer burst will propagate towards the tower tip and, if the average electric field over the streamer length is below the threshold field necessary for streamer propagation, it will stop before bridging the gap. As mentioned earlier, this threshold is different for negative and positive streamers. If the average electric field between the lower tip of the laser filament and the tower tip is larger than the threshold field necessary for streamer propagation, the streamer burst will travel across the whole gap distance between the laser tip and the tip of the tower. This situation is called the final jump condition. In this case, the electrical breakdown between the laser filament and the tower tip is unavoidable, and this generates the conditions necessary for the initiation of a lightning flash. If the average electric field in the gap is below the streamer propagation threshold, still a leader could be generated at the tip of the laser filament and this leader could bridge the gap between the filament and the tower. It is important to point out that if positive streamers from the laser filament cross the gap and initiate a lightning flash, the result will be a positive lightning flash. If negative streamers from the laser filament cross the gap and initiate a lightning flash, the resulting lightning flash will bring negative charge to ground, that is, a negative lightning flash.

Based on the criteria outlined in the previous paragraph, the magnitude of the background electric fields necessary to initiate: (1) a laser-assisted positive lightning flash; (2) a laser-assisted negative lightning flash; and (3) a tower-initiated negative lightning flash without the assistance of the laser filament are estimated. The results are shown as a function of the gap length between the laser filament and the tower tip and for four different lengths of the laser filament in Extended Data Fig. 7. Note that the polarity of the background electric field necessary to initiate a positive lightning flash is opposite to the background electric field necessary to initiate a negative lightning flash. First, observe that the background electric field necessary for the generation of a laser-assisted positive lightning flash is always below the background electric field necessary to initiate a laser-assisted negative lightning flash. Second, observe that at background electric fields that are large enough to initiate a laser-assisted negative lightning flash, the tower itself is capable of generating negative lightning flashes without

the assistance of the laser filament. This also shows that the presence of the laser filament will not substantially change the number of negative flashes striking the tower, but it will make the initiation of positive lightning flashes possible at electric field values which would not allow them in the absence of the laser filament. We have also analysed the maximum gap distance where the laser beam is capable of influencing the lightning initiation. For laser filament lengths equal to 10, 20, 30, 40 and 50 m, the maximum gap lengths where the laser can influence the lightning initiation are 6, 7.5, 20, 22 and 25 m, respectively. The reason why the gap length increases significantly for laser filament lengths larger than 30 m is because for these laser filament lengths, positive leaders are initiated at the laser filament tip and the breakdown is mediated by positive leaders.

Data availability

The datasets generated during and/or analysed during the current study are available from the corresponding author on reasonable request.

References

- Andral, U. et al. Second and third harmonic generation from simultaneous high peak- and high average-power thin disk laser. *Appl. Phys. B* **128**, 177 (2022).
- Pu, Y. et al. Upward negative leaders in positive triggered lightning: stepping and branching in the initial stage. *Geophys. Res. Lett.* **44**, 7029–7035 (2017).
- Saba, M. M. F., Schumann, C., Warner, T. A., Helsdon, J. H. & Orville, R. E. High-speed video and electric field observation of a negative upward leader connecting a downward positive leader in a positive cloud-to-ground flash. *Electr. Power Syst. Res.* **118**, 89–92 (2015).
- Jiang, R., Qie, X., Wang, C. & Yang, J. Propagation features of upward positive leaders in the initial stage of rocket-triggered lightning. *Atmos. Res.* **129**, 90–96 (2013).
- van der Velde, O. & Montanya, J. Asymmetries in bidirectional leader development of lightning flashes. *JGR Atmos.* **118**, 13504 (2013).
- Cooray, V. *Introduction to Lightning* 331–340 (Springer, 2015).
- Cooray, V. in *The Lightning Flash* 2nd edn (ed. Cooray, V.) 41–115 (IET, 2014).
- Bazelyan E. M. & Raizer, Y. P. *Spark Discharge* 145–202 (CRC, 1997)
- Kuffel, E. & Zaengl, W. S. *High Voltage Engineering Fundamentals* 2nd edn, 201–280 (Pergamon, 1984).
- Cooray, V. & Cooray, G. Electromagnetic radiation field of an electron avalanche. *Atmos. Res.* **117**, 18–27 (2012).
- Gallimberti, I. The mechanism of the long spark formation. *J. Phys. Colloq.* **40**, 193–250 (1979).
- Les Renardières Group. Research on long discharges at les Renardières. *Electra* **23**, 53–157 (1972).
- Les Renardières Group. Negative discharges in long air gaps at les Renardières. *1978 Results. Electra* **74**, 67–216 (1981).
- Becerra, M. & Cooray, V. A. Simplified physical model to determine the lightning upward connecting leader inception. *IEEE Trans. Power Deliv.* **21**, 897–908 (2006).
- Arora, R. & Mosch, W. *High Voltage and Electrical Insulation Engineering* 2nd edn, 79–257 (Wiley, 2022).

Acknowledgements

We acknowledge the strong support from M. Pittman, Y. Bertho, IJCLab and University Paris Saclay, who allowed us to perform preparatory experiments with the laser. We also acknowledge the Swiss federal office of Civil Aviation and Swisscom Broadcast AG for their help in the preparation of the lightning campaign at the Säntis Tower, as well as Skyguide and Säntis-Schwebebahn AG for their active cooperation during the campaign. We acknowledge help from R. Bessing and

S. Klingebiel from Trumpf Scientific Lasers with the laser installation, and C. Vassaux, R. Pellet and L. Leuenberger from the mechanical workshops of the University Geneva for the construction and installation of the telescope housing. We acknowledge the European Union Horizon 2020 Research and innovation programme FET-OPEN grant (grant no. 737033-LLR to all authors), the Swiss National Science Foundation (grant no. 200020-175594 to A.S., A. Mostajabi, M.R. and F.R.), the Swiss National Science Foundation (grant no. 200021-178926 to U.A., M.S. and J.-P.W.), the French Direction Générale de l'Armement (to L.B., P.W., Y.-B.A.), and B. John F. and S. Andersson's donation at Uppsala University (V.C.).

Author contributions

J.-P.W., A.H., A.M.Y., J.K., F.R. and M.R. initiated and defined the project. A.H., J.-P.W., A.M.Y., T.M., B.E., F.R. and M.R. obtained funding and supervised the project. A.H. coordinated the project. T.P., U.A., G.S., M.M., J.K., J.-P.W., B.M., P.W., A.H. and W.H. designed and installed the experiment. A.S., F.R. and M.R. designed and installed the lightning experiment. P.W., T.P., B.M., V.M., U.A., J.K., J.-P.W., Y.-B.A., M.L., L.B., A.H. and M.C.S. conducted the laser experiments on site. A.S., A.M.O., M.R., F.R., O.M., M.S. and W.A.R. conducted the lightning experiment and characterization. C.H., K.M. and T.M. developed the laser system. V.C. developed the lightning simulations. P.W., A.S., J.-P.W., J.K., V.M.

and W.A.R. analysed the data. A.M.Y. and A.H. prepared the original draft, and all authors critically reviewed and approved the manuscript.

Competing interests

The authors declare no competing interests.

Additional information

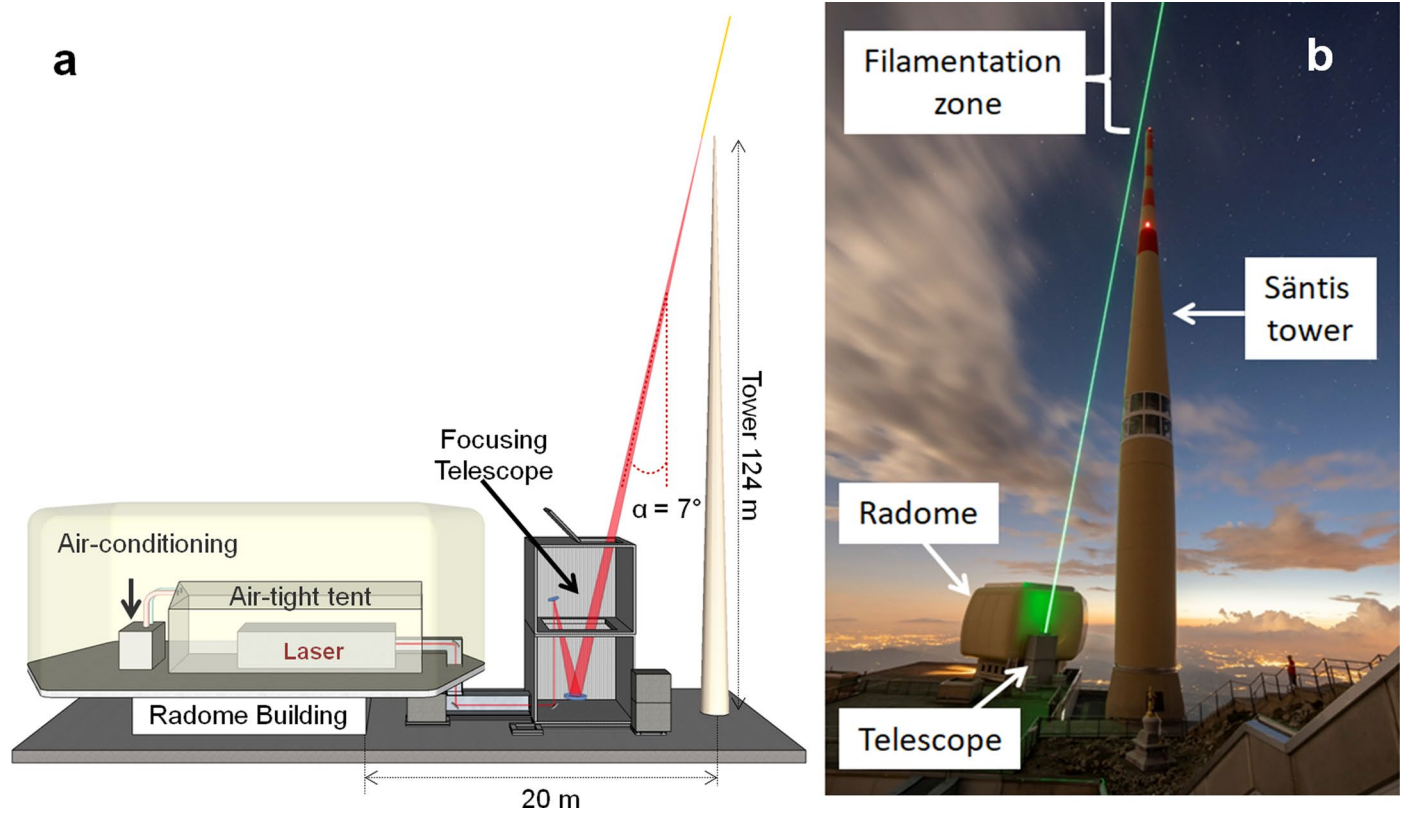
Extended data is available for this paper at <https://doi.org/10.1038/s41566-022-01139-z>.

Supplementary information The online version contains supplementary material available at <https://doi.org/10.1038/s41566-022-01139-z>.

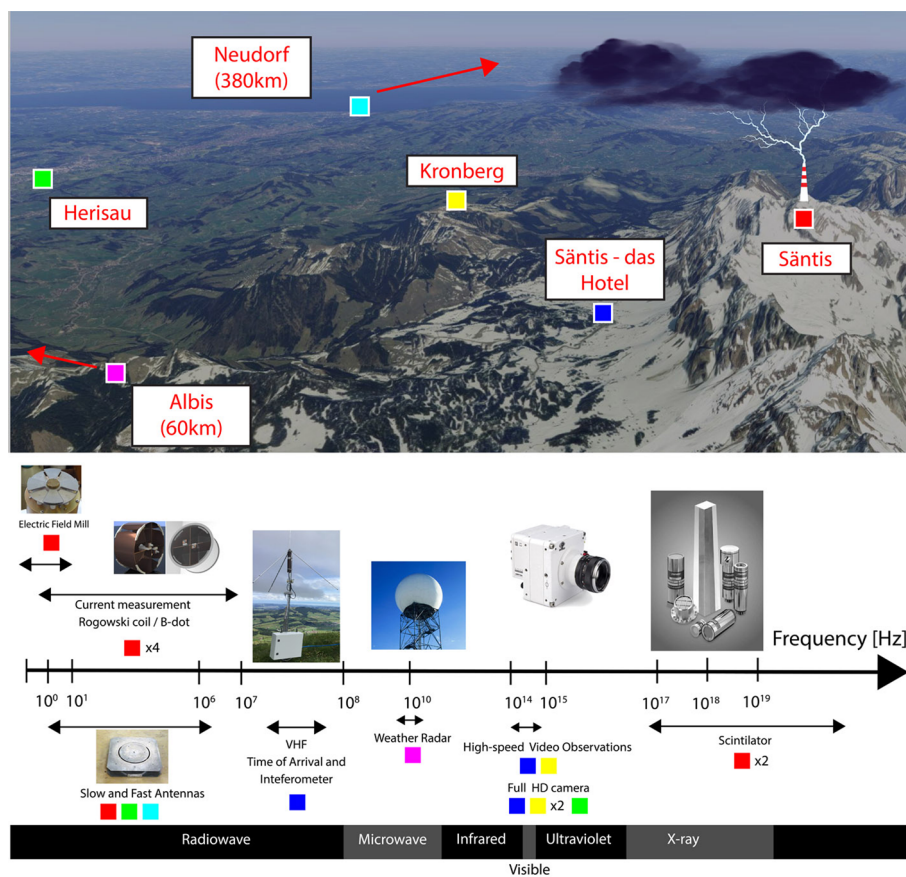
Correspondence and requests for materials should be addressed to Aurélien Houard or Jean-Pierre Wolf.

Peer review information *Nature Photonics* thanks Olga Kosareva and the other, anonymous, reviewer(s) for their contribution to the peer review of this work.

Reprints and permissions information is available at www.nature.com/reprints.

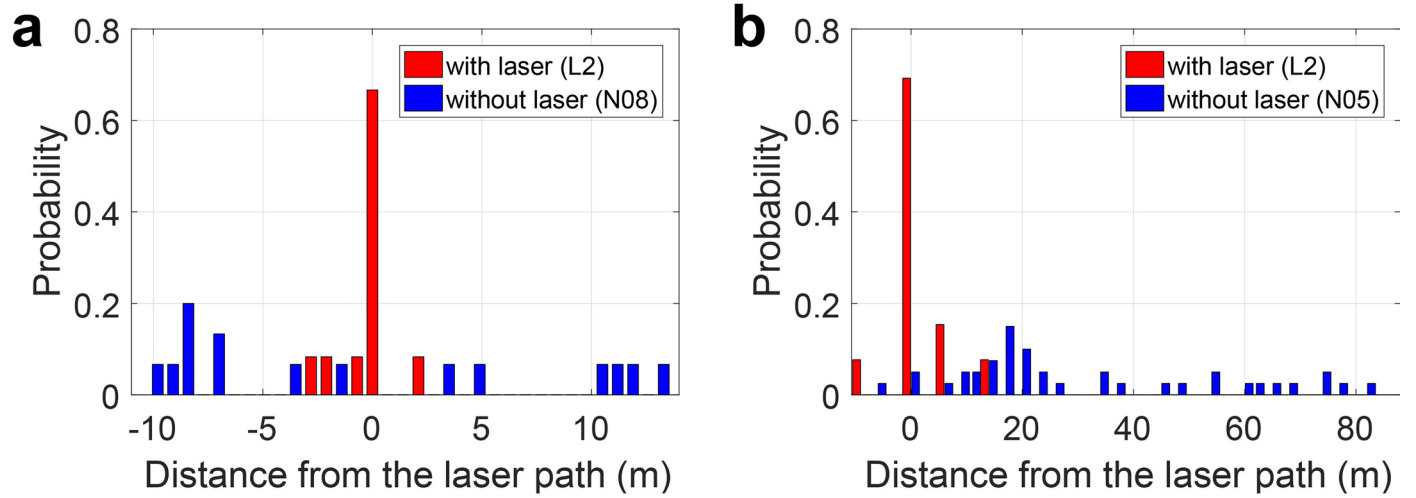


Extended Data Fig. 1 | Experimental set-up. **a**, Layout of the experimental setup on top of the Säntis Mountain. **b**, Photography of the experiment with the second harmonic of the laser beam used to visualize the laser path.

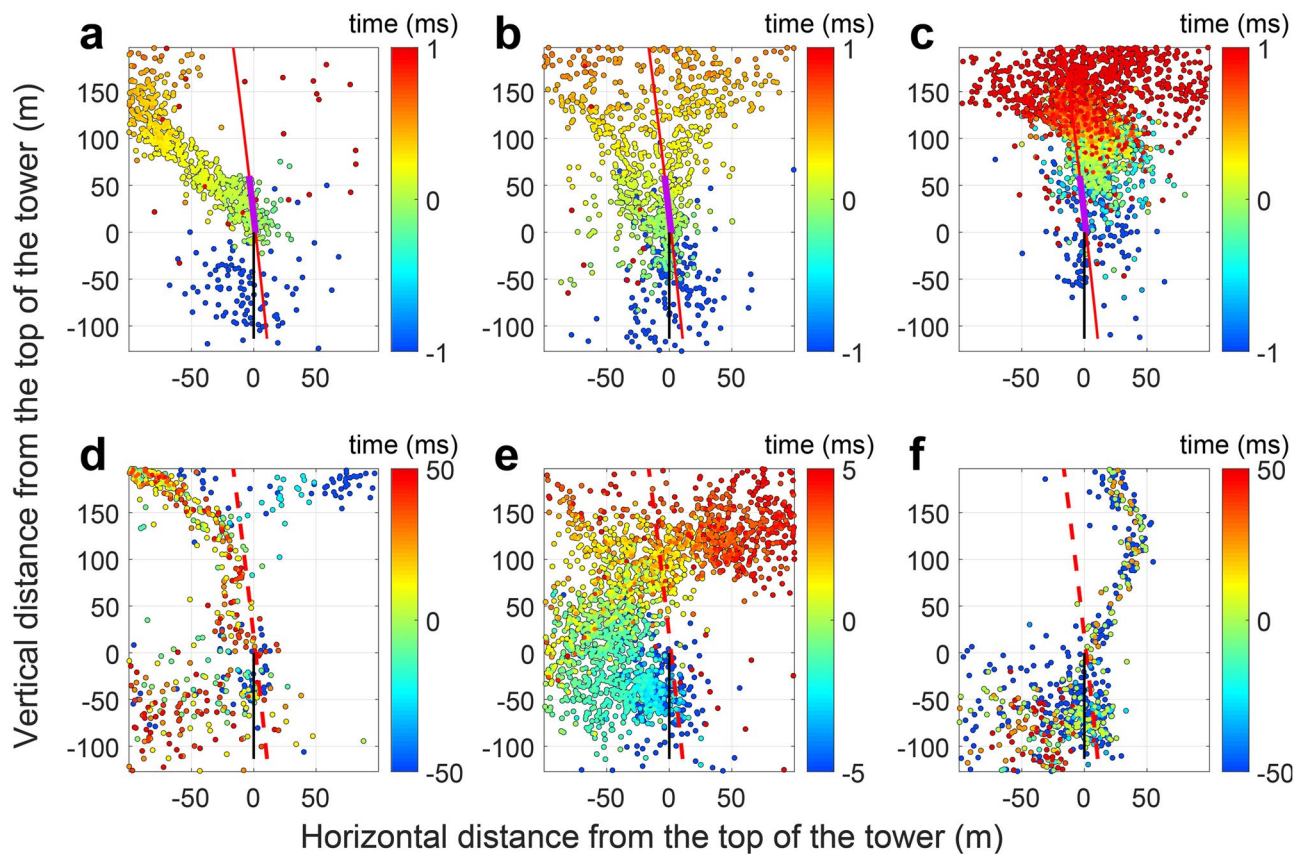


Extended Data Fig. 2 | Locations of the different measuring equipments. The Sântis lightning measurement system consists of two fast electric field sensors, a field mill, three full HD cameras, two high speed cameras and two X-rays sensors. Data from the weather radar covering the Sântis Tower area are also made available by MeteoSwiss. Lightning currents of strikes to the tower were measured by a set of Rogowski coils and B-dot sensors located at two different heights along the tower (see refs. 32, 34 for more information on the Sântis Tower instrumentation). The lightning activity was detected, located in azimuth and elevation, and GPS-time-stamped by a radiofrequency interferometer in the 1–160 MHz band³⁸ whose upper cutoff was limited to 84 MHz to avoid

interference from FM radio transmitters in the area. We checked that, without electric activity in the atmosphere, the interferometer is fully insensitive to the laser system and to the laser induced filaments. An X-ray detector located in the radome measured the X-rays emitted in the range 20 keV–1 MeV. Electric field measurements were performed 20 m and 15 km away from the tower. Finally, two high-speed cameras were installed from two viewing angles to provide direct imaging of the lightning strikes in case of clear weather under elevated thunderclouds. Located in Schwägalp and Kronberg, they operated, respectively, at 10,000 and 24,000 frames per second.

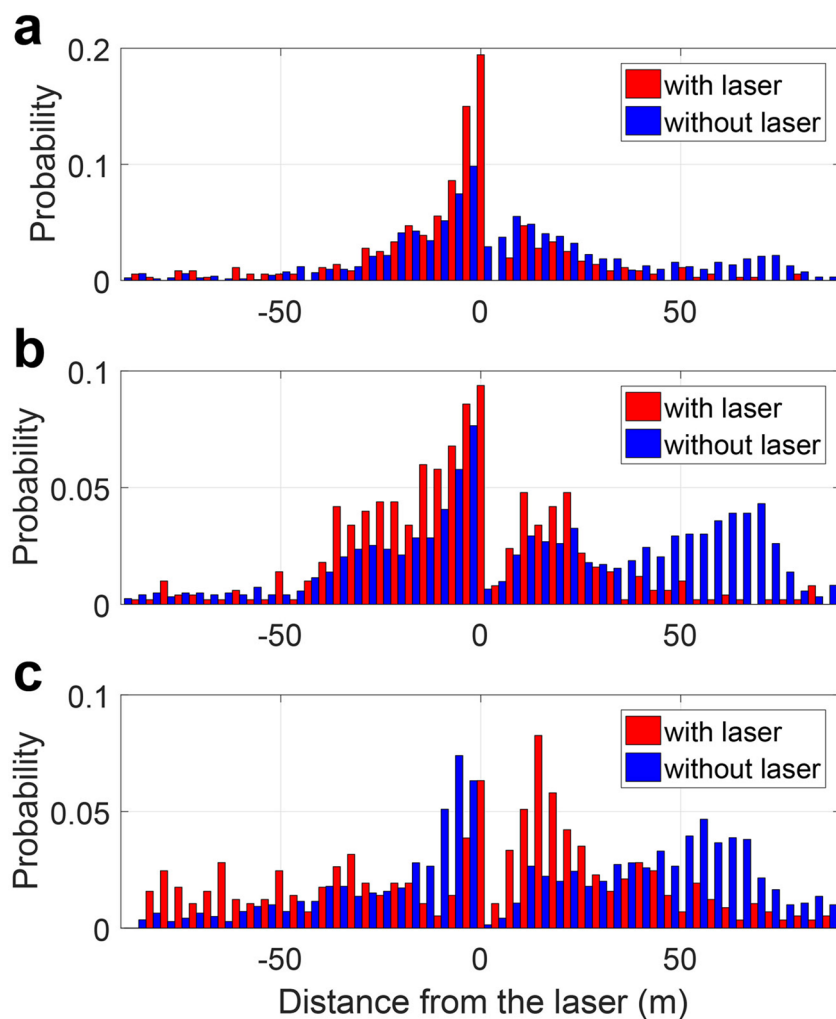


Extended Data Fig. 3 | Analysis of high-speed camera measurements. Projected 2D histograms based on single image, comparing **a**, event L2 with N08 viewed from Sántis, and **b**, L2 with N05 viewed from Kronberg.



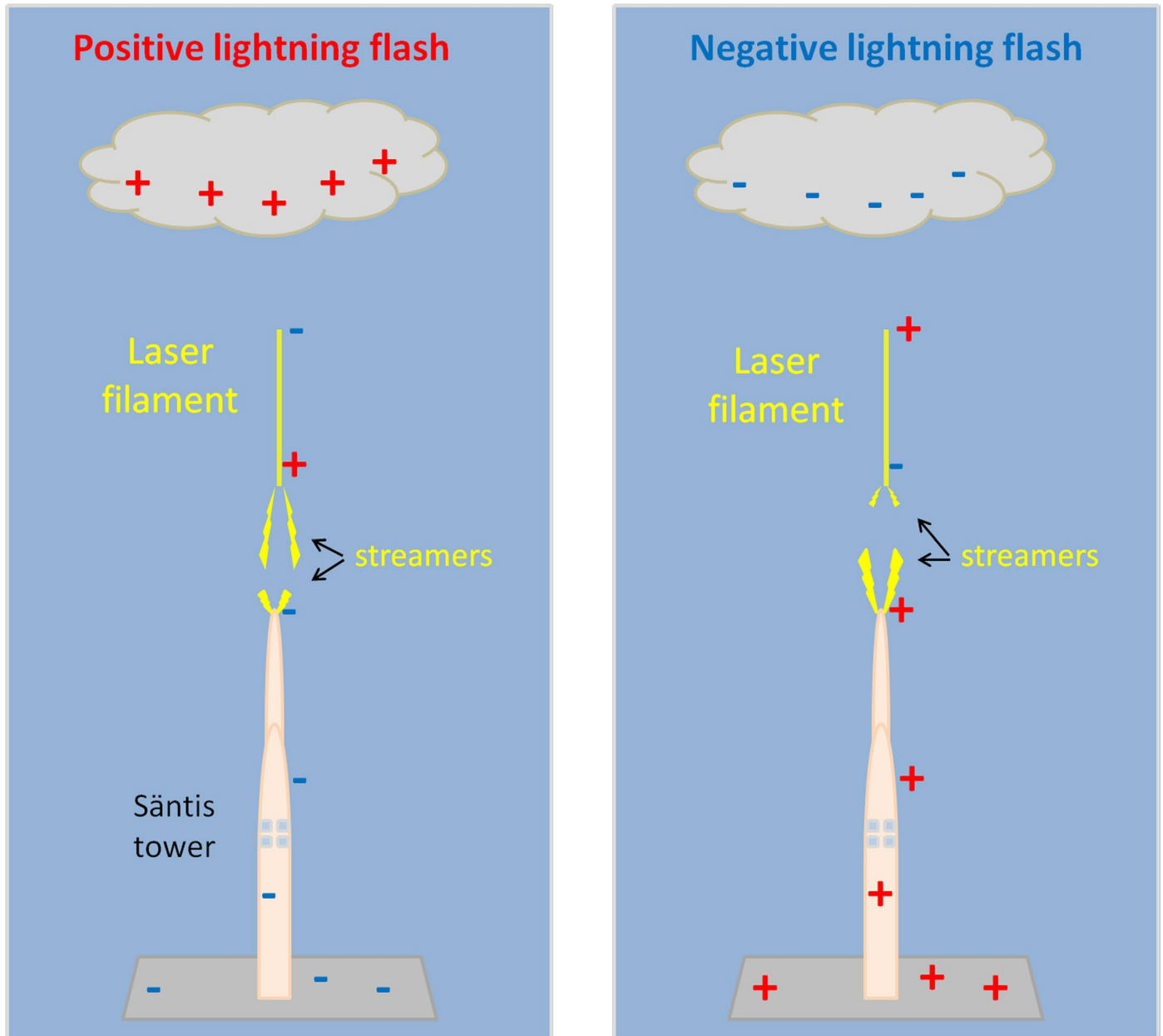
Extended Data Fig. 4 | VHF sources position. Still images could be obtained in only one lightning strike while the laser was flashing, due to the exceptional visibility conditions required. In contrast, the RF interferometer also displays guiding for the 3 recorded events with laser (L1, L3, L4), in the form of a high density of VHF sources close to the laser beam. Typical results with laser (events L1, L3, L4) are presented respectively in panels **a–c**. Events without laser (N02, N06, N07) in panels **d–f**. Each panel displays 2D (vertical and horizontal distances

from the top of the tower) maps of the sources constituting lightning strikes on the tower. The colour code displayed on the right corresponds to the timescale. The Sântis Tower is represented on each plot in black, the laser path in red, and the part of the laser path over which filaments are expected in violet. The dashed red line in the lower panels represents the path that the absent laser beam would have followed.

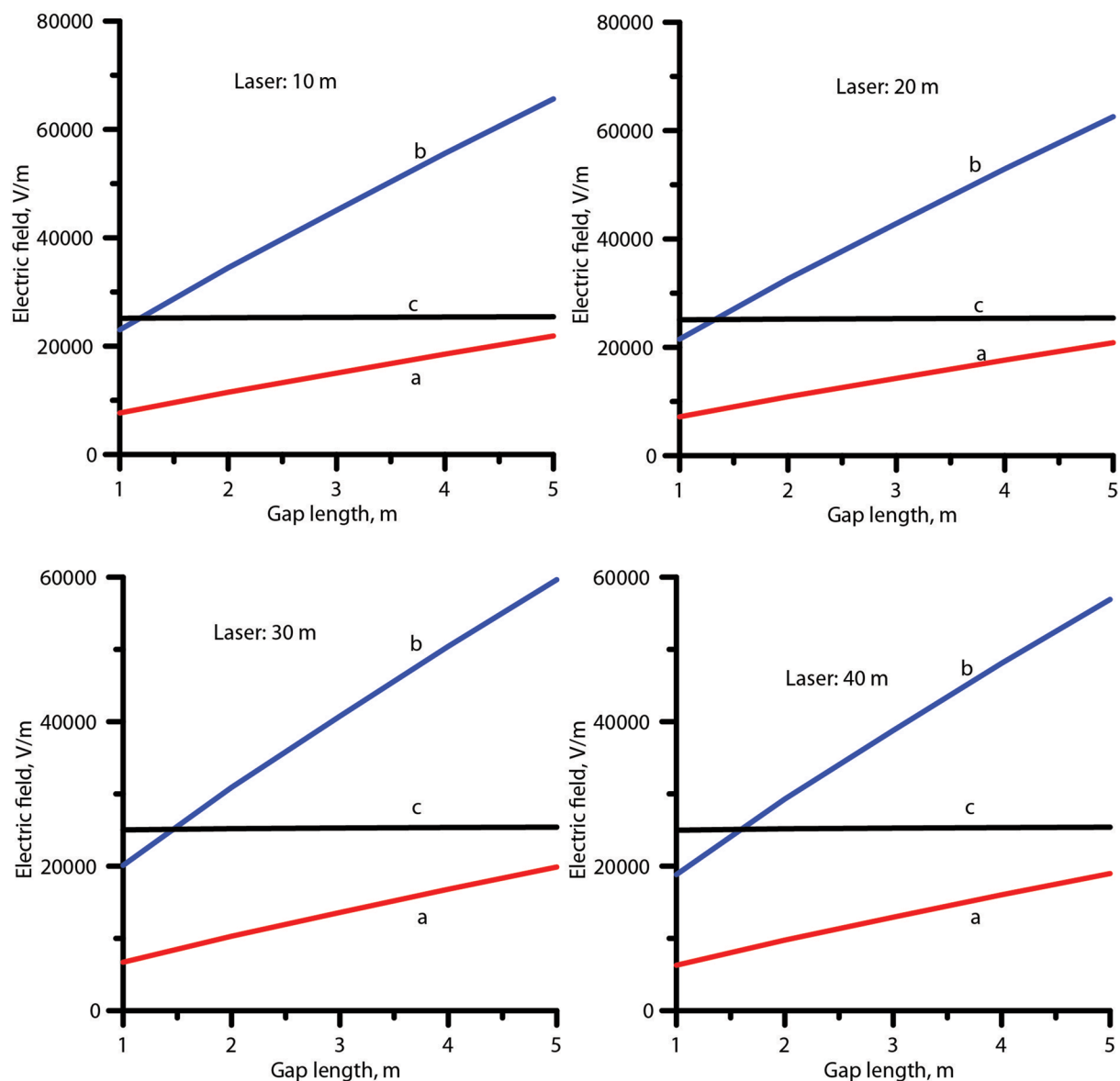


Extended Data Fig. 5 | Histograms of VHF source distance to the laser beam. Comparison of the cumulated histograms of distance to the laser beam per height slice of 30 m for all events with and without laser. **a**, **b** and **c** correspond

respectively, to the height slices 0–30 m, 30–60 m, and 60–90 m. When the laser is on, the distribution is centred closer to the laser beam, and narrower, as compared to when the laser is off.



Extended Data Fig. 6 | Geometry considered for the simulation. The laser filament is assumed to be located vertically and directly above the tower tip. Left panel: conditions associated with a positive flash. Right panel: conditions associated with a negative flash.



Extended Data Fig. 7 | Simulation of the effect of laser filamentation on the lightning flashes initiation. Magnitude of the background electric fields necessary to initiate laser assisted positive lightning flashes (red curves marked 'a') and laser-assisted negative lightning flashes (blue curves marked 'b'), as a function of the gap length between the lower tip of the laser filament and the tower tip. The curves marked 'c' depict the magnitude of the background electric field necessary for the tower to initiate a negative lightning flash without the

assistance of the laser filament. The lengths of the laser filament used in the calculation are given in each diagram. Note that the polarity of the background electric field necessary to initiate a positive lightning flash is opposite to the background electric field necessary to initiate a negative lightning flash. The field presented is not the total field but the background electric field. The absolute electric field at the tower tip is enhanced due to the presence of the tower by a factor of 50 to 100.

Extended Data Table 1 | Lightning strike events during the campaign, and available diagnostics for each event

Events	Date	UTC Time	Laser	Current	Flash polarity	HSC	INT	X-RAY	E (20m)	E (15km)
L1	24.7.2021	16:06:07	ON	YES	POS	NO	YES	YES	YES	YES
L2	24.7.2021	16:24:03	ON	YES	POS	YES	NO	YES	YES	YES
L3	30.7.2021	18:00:10	ON	YES	POS	NO	YES	YES	YES	YES
L4	30.7.2021	18:02:40	ON	YES	POS	NO	YES	NO	NO	YES
N01	30.7.2021	15:17:09	OFF	YES	NEG	NO	YES	YES	YES	YES
N02	30.7.2021	15:22:29	OFF	YES	NEG	NO	YES	NO	NO	NO
N03	30.7.2021	15:30:51	OFF	YES	NEG	NO	YES	YES	YES	NO
N04	30.7.2021	15:35:41	OFF	YES	NEG	NO	YES	YES	YES	YES
N05	30.7.2021	15:38:10	OFF	YES	NEG	YES	YES	YES	YES	YES
N06	30.7.2021	18:04:53	OFF	YES	POS	NO	YES	YES	YES	YES
N07	16.8.2021	02:00:27	OFF	YES	NEG	NO	YES	NO	NO	NO
N08	16.8.2021	02:34:10	OFF	YES	NEG	YES	YES	YES	YES	YES
N09	16.8.2021	05:53:24	OFF	YES	NEG	NO	YES	YES	YES	YES
N10	16.8.2021	10:16:32	OFF	YES	NEG	NO	YES	NO	NO	NO
N11	16.8.2021	15:06:45	OFF	YES	NEG	NO	YES	YES	YES	NO
N12	16.8.2021	15:08:34	OFF	YES	NEG	NO	YES	YES	YES	NO

Sixteen flashes were recorded by the current measuring system at the Sântis Tower during the experimental campaign from 21 July to 30 September 2021. Due to both the harsh experimental conditions as well as intrinsic instrument limitations (optical visibility, buffer size and electromagnetic perturbations), each event could not be recorded by all instruments. The status of the laser system and each measuring system, including a high-speed camera (HSC), an interferometer (INT), X-rays sensors (X-ray), an electric field 20m from the tower (E-field (20m)) and an electric field 15 km from the tower (E-field), for each of these events is given in Table 1. Five out of the 16 flashes were positive (POS), whereas eleven were negatives (NEG). Only three were recorded by at least one high-speed camera (two without laser and one with the laser on), whereas all but one were recorded by the interferometer. All investigated lightning strikes were of the upward type, like 97% of the strikes observed at Sântis since 2010³⁶. All four recorded laser events were positive; by contrast, 85% negative flashes, 12% positive flashes and 3% bipolar flashes were recorded during the summer of 2021. Assuming conditions during the campaign similar to the average of the ten previous years, the excess of positive flashes when the laser is on is significant beyond 10^{-3} (P -value= 6.7×10^{-6} obtained with unilateral χ^2 test).

Extended Data Table 2 | Standard deviation of the VHF source distance to the laser beam

Elevation (m)	laser	Number of sources	Standard deviation (m)
00-30	OFF	1644	39.7
	ON	586	24.2
30-60	OFF	1502	46.0
	ON	778	26.4
60-90	OFF	1674	44.1
	ON	738	39.6
00-60	OFF	3146	42.7
	ON	1364	25.5

Using the data presented in Extended Data Fig. 5, we calculated the standard deviation of this distance for different elevations above the tower. For all three height slices, we performed a unilateral F-test. For the whole 0–90 m range, the standard deviations of the histograms are significantly different (P -value $\ll 10^{-15}$), that is, histograms with the laser turned off are more dispersed. Considering the 0–60 m range, we find that the standard deviation of the distance of the sources to the laser is reduced by 45% when the laser is on. Above 60 m, this reduction due to the laser filament is much weaker, as expected since the length of the filament is estimated to be 50–60 m.